Original Article

Active targeted nanoparticles: Preparation, physicochemical characterization and *in vitro* cytotoxicity effect

Sh. Heidarian[1], K. Derakhshandeh[1,2,*], H. Adibi[3] and L. Hosseinzadeh[4]

[1]Department of Pharmaceutics, Faculty of Pharmacy, Kermanshah University of Medical Sciences and Nano Technology Research Center, Kermanshah, I.R. Iran.
[2]Nano Drug Delivery Research Center, Kermanshah University of Medical Sciences, Kermanshah, I.R. Iran.
[3]Department of Medicinal Chemistry, Faculty of Pharmacy, Kermanshah University of Medical Sciences, Kermanshah, I.R. Iran.
[4]Department of Pharmacology and Toxicology, Faculty of Pharmacy, Kermanshah University of Medical Sciences, Kermanshah, I.R. Iran.

Abstract

In this study, the folate decorated biodegradable poly (lactide-co-glycolide) (PLGA) nanoparticles were developed for tumor targeting of anticancer agents. Due to the overexpression of the folate receptor on tumor surface, the folate has been efficiently employed as a targeting moiety for various anticancer agents to avoid their non-specific attacks on normal tissues and also to increase their cellular uptake within target cells. Folate conjugate PLGA was synthesized successfully and its chemical structure was evaluated by FTIR, DSC and ^{1}HNMR spectroscopy. PLGA-folate nanoparticles (PLGA-Fol NPs) were prepared by nanoprecipitation method, adopting PLGA as a drug carrier, folic acid as a targeting ligand and 9-nitrocampthotecin as a model anticancer drug. The average size and encapsulation efficiency of the prepared PLGA-Fol NPs were found to be around 115 ± 12 nm and 57%, respectively. *In vitro* release profile indicated that nearly 85% of the drug was released in 50 h. The *in vitro* intracellular uptakes of PLGA-Fol NPs showed greater cytotoxicity on cancer cell lines compared to non-folate mediated carriers.

Keywords: 9-Nitrocamptothecin; PLGA-Fol nanoparticles; Targeting drug delivery; *In vitro* cytotoxicity

INTRODUCTION

Folate is essential for the production and maintenance of new cells. Many cancer cells have higher demand for folic acid (1,2). In the form of a series of tetrahydrofolate compounds, folate derivatives are substrates in a number of single-carbon-transfer reactions, and also are involved in the synthesis of 2′-deoxythymidine-5′-phosphate (dTMP) from 2′-deoxyuridine-5′-phosphate (dUMP). It is a substrate for an important reaction that involves vitamin B_{12} and it is necessary for the synthesis of DNA required for all dividing cells (3,4). Normal cells transport the folates across the plasma membrane by two membranes-associated proteins, the reduced folate carrier and the folate receptor. The folate receptor is a glycosyl phosphatidyl inositol-linked membrane glycoprotein. Two membranes-bound isoforms of folate receptor have been identified in humans, α and β (4,5).

The elevated folate receptor expression has been observed in ovarian, endometrial, breast, renal cell carcinoma, lung and brain metastases (6,7). The receptor-mediated endocytosis is an attractive mechanism for the cell-selective drug targeting, since this process exhibits high transport capacity and ligand-dependent cell specificity (4).

Therefore, folate receptor is considered to be a good candidate for tumor-specific targeting. In tumor cells, this uptake allows over 10^6 conjugate molecules to enter the cell per h (7,8). Although the internalization of these conjugates occurs via a receptor-mediated pathway, it could be competitively blocked by the excess of free folate (8-10).

The application of the folate targeting for macromolecular delivery to cancer cells is

*Corresponding author: K. Derakhshandeh
Tel: 0098 831 4276482, Fax: 0098 831 4276482
Email: kderakhshandeh@kums.ac.ir

classified into two categories. For drugs that require an intracellular release to exert their cytotoxic functions, folate receptor offers a ligand-activated endocytosis for transporting into the cytoplasm of cancer cells (6). Protein toxins, oligonucleotides, liposomes, and many other colloidal drug carriers are the examples of macromolecules that exist in this category (11-13).

On the other hand, for drugs that do not need intracellular loading, and have cytotoxic functions on the surface of a target cell, folate receptor can act as a tumor marker and lead to the release of the drug on the cell surface.

The attraction of folate has been further enhanced by its high binding affinity low immunogenicity, ease of modification, small size, stability during storage, compatibility with a variety of organic and aqueous solvents, low cost, and ready availability (12).

Therefore, in this study, we have developed the folate-decorated biodegradable poly (lactide-co-glycolide) (PLGA) nanoparticles (NPs) for targeted delivery of a potent anticancer drug, 9-Nitro-20(*S*)-camptothecin (9-NC). 9-NC, an analog of camptothecin, which is a promising broad-spectrum anticancer agent with high potency against human cancers, and has achieved remarkable success in early clinical trials (14,15). The unstable lactone form of 9-NC in biological fluids requires the cytotoxic activity of the drug (Fig. 1). Until recently, we have formulated different PLGA and PLGA-PEG passive targeting nanocarriers of this drug (16-18). The results showed that incorporation of this labile drug in nanocarriers could enhance its stability and also modify its dissolution characteristics. In the present study, we

decided to incorporate the drug in the core of the folate-decorated NPs for its active targeting to specific cells.

The PLGA-folate nanoparticles (PLGA-Fol NPs) were prepared by nanoprecipitation method and characterized in terms of surface morphology, particle size, drug encapsulation efficiency (EE) and *in vitro* drug release in the present study. The *in vitro* cytotoxicity of NPs on different cell lines was also investigated.

MATERIALS AND METHODS

Materials

9-Nitrocamptothecin with 99.8% purity was purchased from Yuanjian Pharmaceutical Technology Develop Co, (China). PLGA, (75:25 MW 12000), 3-(4,5-dimethylthiazol-z-yl)-2,5-diphenyl tetrazolium bromide (MTT), Trypsin- ethylenediaminetetraacetic acid, N, N-dicyclo- hexylcarbodiimide (DCC), N-hydroxysuccinimide (NHS), Folate, pyridine, ethylene diamine (EDA) analytical grade acetone, and potassium dihydrogen phosphate were supplied by Merck (Darmstadt, Germany).

Polyvinyl alcohol (PVA, MW 30000 Da, 87% hydrolyzed) was a gift from Mowiol (Germany). Dichloromethane (DCM) and dimethyl sulfoxide (DMSO, anhydrous) were procured from Sigma-Aldrich (St. Louis, USA).

Synthesis of PLGA-Fulic acid (PLGA-Fol)

PLGA-Fol was synthesized using a modified method already described (19). Five hundred mg PLGA was activated by DCC and NHS in 10 ml DCM (PLGA/DCC/NHS molar ratio = 1:1.1:1.1) at room temperature under nitrogen gas for 24 h.
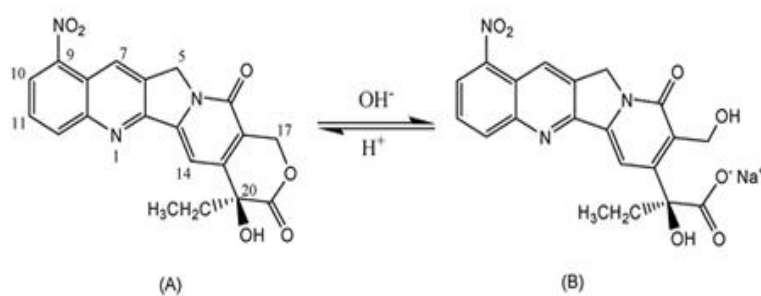

Fig. 1. Chemical structures and equilibrium reaction between the lactone and carboxylate forms of 9-NC.
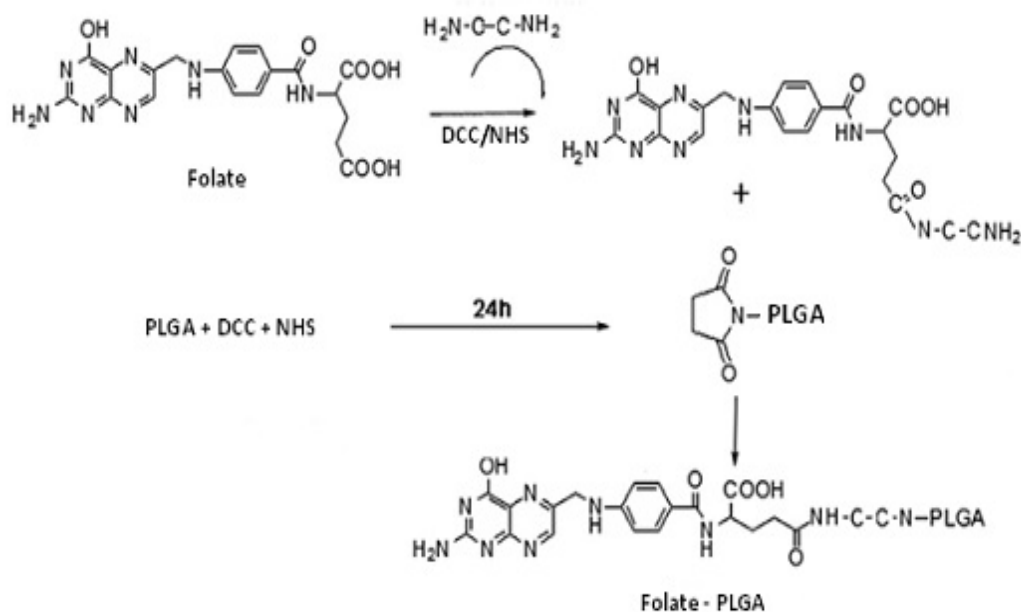
Fig. 2. Synthesis of PLGA-Fol copolymer.

The folate was activated using DCC and NHS in the presence of 10 µl pyridine (folate/NHS/DCC molar ratio = 1:1.1:1) and reacted with 0.5 g EDA in 5 ml DMSO. Conjugation of Folate-NH$_2$ with the activated PLGA was performed in DMSO at room temperature for 48 h under nitrogen gas (Fig. 2).

The chemical structure of the synthesized PLGA-Fol was characterized by Fourier transformed-infrared spectroscopy (FTIR) and Proton Nuclear Magnetic Resonance (^{1}H NMR) spectroscopy and coupling of the folate to PLGA was proved.

Preparation of nanoparticles

NPs were prepared by the nanoprecipitation method (16-18). In brief, PLGA-Fol and the drug were dissolved in acetone and then the solution was added drop-wise into the aqueous solution containing PVA (pH was adjusted to 3 using 0.1 N HCl) under magnetic stirring. Acetone was evaporated at room temperature and NPs were separated using ultracentrifuge (Beckman XL 90, USA) at 30000 rpm for 30 min. NPs were then washed thrice in order to remove free drug and excess surfactant completely. The precipitated NPs were freeze-dried and kept for further experiments.

Structural characterization of 9-NC loaded PLGA-Fol NPs

Size, zeta potential, and morphology characterization

The morphology and structure of the NPs were examined using a transition electron microscope (Zeiss-EM 10C-Germany) at an accelerating voltage of 80 kV and 0.3 nm (point-to-point). For analysis, the samples were placed on the copper grids for observation. For obtaining TEM image the freshly prepared NPs were investigated.

The measurement of the hydrodynamic diameter, polydispersity index, and zeta potential of the NPs was accomplished using the photon correlation microscopy (PCS) (Nano ZS4700, Malvern Instruments, Worcestershire, UK). For the size and zeta potential measurement, all formulations were diluted with deionized water to eliminate the effect of viscosity caused by the ingredients.

The thermal characteristics of the 9-NC and the folate in PLGA NPs were assessed using a differential scanning calorimeter (DSC-60, Shimadzu Co. Kyoto, Japan) under a dry nitrogen atmosphere. The samples (8 mg) were placed in an aluminum pan and heated at a rate of 10 °C/min, and empty indium pans were used as references.

Encapsulation efficiency and in vitro drug release profile

The entrapment efficiency (EE) was determined spectrophotometrically at 370 nm using a Schimadzu UV-Vis spectrophotometr (UV MINI-1240, Japan) after ultra-sonication of the aqueous dispersion (20 mg of samples was dissolved in 4 ml acetone). The drug entrapment efficiency was calculated using following equation (1):

$$EE\% = \frac{W_1}{W_2} \qquad (1)$$

where, W_t and W_l are the weight of the drug added into the system and the amount of 9-NC in NPs, respectively.

To determine the *in vitro* drug release profile, 9-NC-loaded NPs were placed into a dialysis membrane (molecular weight cutoff 12000 KDa) and immersed in 2 ml phosphate buffer solution (PBS) in diffusion cell that was gently shaken at 100 rpm at 37 $^{\circ}$C. At determined interval times, the PBS solution was refreshed and the concentration of 9-NC remained in the dialysis cell was measured using UV spectrophotometer.

To determine the mode of drug release, the initial 60% drug release values were fitted to the Korsmeyer-Peppas model:

$$\frac{M_t}{M_\infty} = Kt^n \qquad (2)$$

where, M_t/M_∞ is the fraction of drug released at time t, K is the drug release rate constant, and n is the release exponent. The n value is employed for the characterization of different release modes for cylindrical-shaped solid formulations. The drug release exponent (n) and drug release mode are related as: n = 0.45, Fickian diffusion; 0.45< n <0.89, Anomalous (non-Fickian) diffusion; n = 0.89, Case-II transport; and n >0.89, Super case-II transport (20).

Fourier transformation infrared spectroscopy characterization of nanoparticles

The FTIR spectra were obtained using Schimadzu IR-prestige 21 FTIR spectrometer. To measure the FT-IR spectrum of NPs, 2 mg of the samples were mixed with 10 mg KBr and compressed to make tablets. The IR spectra of these tablets were obtained in an absorbance mode and in the spectral region of 450 to 4,000 cm^{-1}.

In vitro cytotoxicity assay

The cell lines were transferred to 96-well tissue cultured plates for 24 h prior to the drug release. Then the medium was replaced with the fresh medium containing blank and the drug loaded NPs at different concentration. The culture medium without any drug formulation was used as the control. After 24 h, 200 μl MTT (0.5 mg/ml) was added to each well and incubated for 3 h at 37 $^{\circ}$C. The medium was then removed and 100 μl DMSO was added to dissolve the blue formazan crystal obtained from MTT. The cell viability was measured at 490 nm in a micro plate reader.

Human-breast adenocarcinoma (MCF-7), human colon adenocarcinoma (HT-29), human prostate adenocarcinoma (PC-3), rat cardiomyoblast cell (H9C2) and human Umbilical Vein Endothelial Cells (HUVEC) were used as the cell lines in this research.

RESULTS

Synthesis of PLGA-Fol

The principle goal of the chemical reactions in the synthesis of PLGA-Fol is the formation of the amide bond. The conjugation was checked and confirmed by FTIR and ^{1}H NMR spectroscopy as shown in Fig. 3 and 4. FTIR spectrum of pure folate, polymer and modified polymer were obtained.

The spectrum of modified PLGA (Fig. 3) proved the conjugation quantitatively by several characteristic vibration bands. The band around 1633 cm^{-1} was assigned to amidic -C=O stretching vibration and the band around 1576 and 3357 cm^{-1} was attributed to the characteristic absorption of the N-H in amide bond in folate modified PLGA.

Also the peak around 1750 cm^{-1} belongs to steric group in the polymer. ^{1}H NMR analysis (Fig. 4) showed principal peaks (in ppm) related to the benzene of the folate moiety [δ= 6.65, 6.8, 7.7, 7.88 ppm].

The PLGA groups moiety (CH$_3$, CH$_2$ and CH) are shown in δ=1-2 and 4.7–5 ppm. Also the peak between 6-7 ppm, indicated amidic hydrogen. All these results showed the successful interaction of the folate with PLGA.
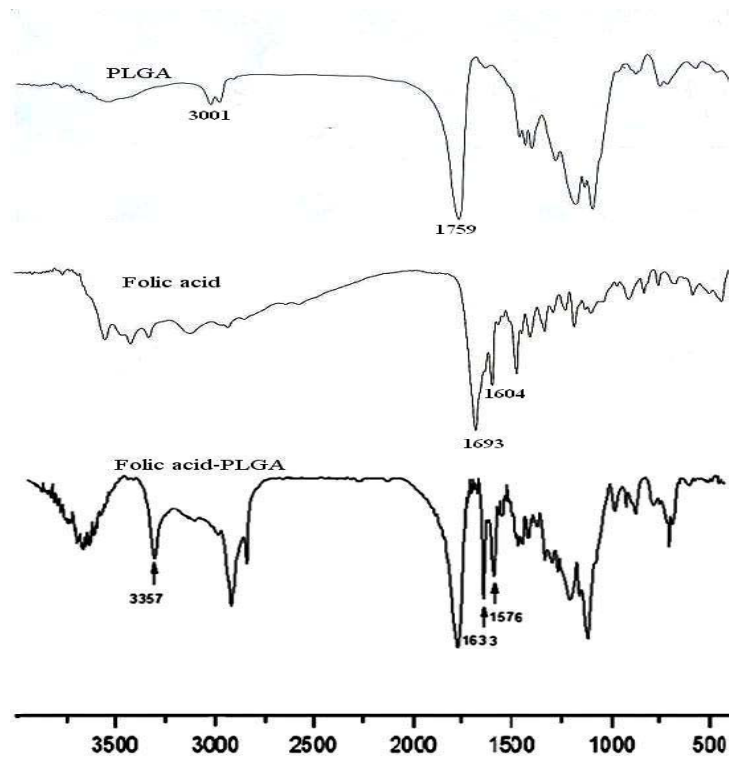
Fig. 3. The FTIR spectrum of Folic acid, PLGA and PLGA-Fol copolymer.
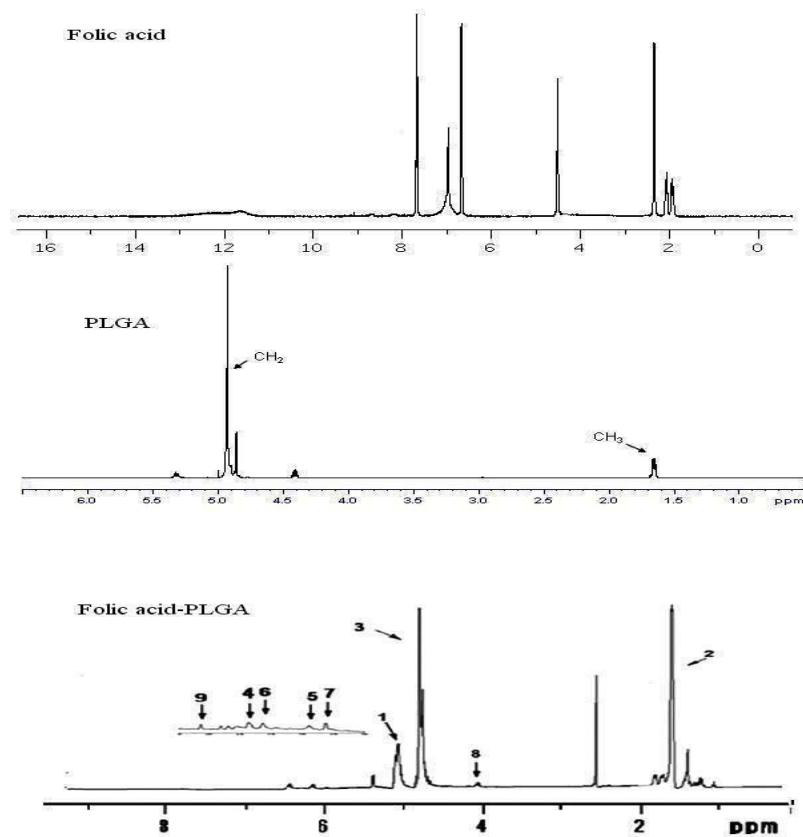

Fig. 4. The ^{1}H-NMR spectrum of Folic acid, PLGA and PLGA-Fol copolymer.

Optimizing formulation of 9-NC PLGA and PLGA-Fol NPs

Several formulations were prepared and characterized for particle size, size distribution, surface charge, and morphology and encapsulation efficiency to achieve optimal formulation. In these formulations, the volume of internal to external phase, emulsifier and of polymer amount were optimized (Table 1).

Characterization of PLGA-Fol NPs

PCS measurement showed that the mean diameter of PLGA-Fol NPs for formulation 4 was around 115 ± 12 nm with a polydispersity index of 0.32. The mean diameter of PLGA NPs was 94 ± 17 nm with a polydispersity index of 0.24. The increment of the particle size for PLGA-Fol NPs compared to PLGA NPs was presumably due to the presence of the folate fragment on the NPs surface. Also the TEM micrographs (Fig. 5) of NPs showed that the NPs had a spherical morphology with a particle size in nanometric range. The particle size of the PLGA NPs depicted in TEM images is in agreement with the results obtained with PCS.

Zeta potential is a key factor for evaluation of the stability of a colloidal dispersion. The high surface potential of the suspension reduces the cohesion between the particles, and the particles are likely to be electrochemically stable under the investigated condition after preparation (21). The folate-decorated PLGA NPs had a more negative zeta potential (-17.4 mV) compared with the surface charge of unmodified NPs (-12.3 mV). This is due to the protonated amino acid groups of the folate. The absolute amount of the zeta potential of prepared NPs is high, and it could guarantee the stability of the particles after preparation.The differential scanning calorimetric thermograms for pure 9-NC, folate, and polymer, physical mixture of drug-polymer and drug-folate, PLGA and PLGA-Fol NPs are shown in Fig. 6.

Table 1. Optimum formulation of PLGA and PLGA-FOL nanoparticles loaded 9-NC.

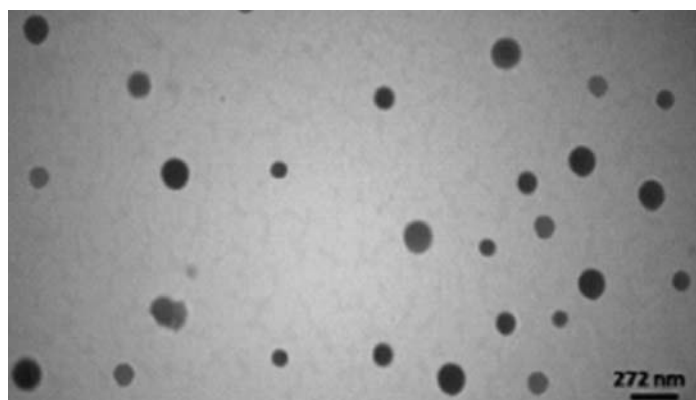| Composition	Polymer (mg)	Emulsifier (mg)	Internal phase (ml)	External Phase (ml)	Folate linkage (%)	EE (%)
PLGA	165	28	12	21.33	-	32
PLGA-FOL	125	50	18	4	17	21
PLGA-FOL	150	50	18	10	17	32.4
PLGA-FOL	167.25	27.94	21.33	12	17	57

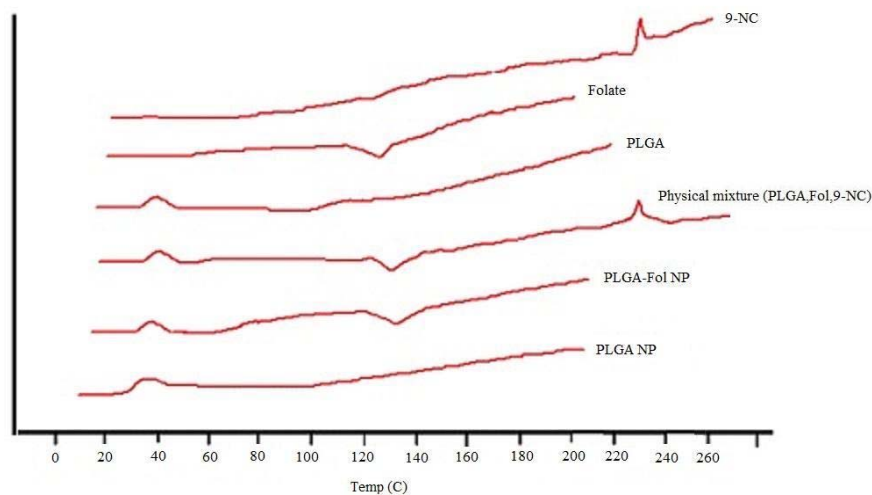**Fig. 5.** Transmission electron micrograph of PLGA-Fol NPs.

Fig. 6. DSC thermograms of drug, folate, polymer, their physical mixture, and nanoparticles.
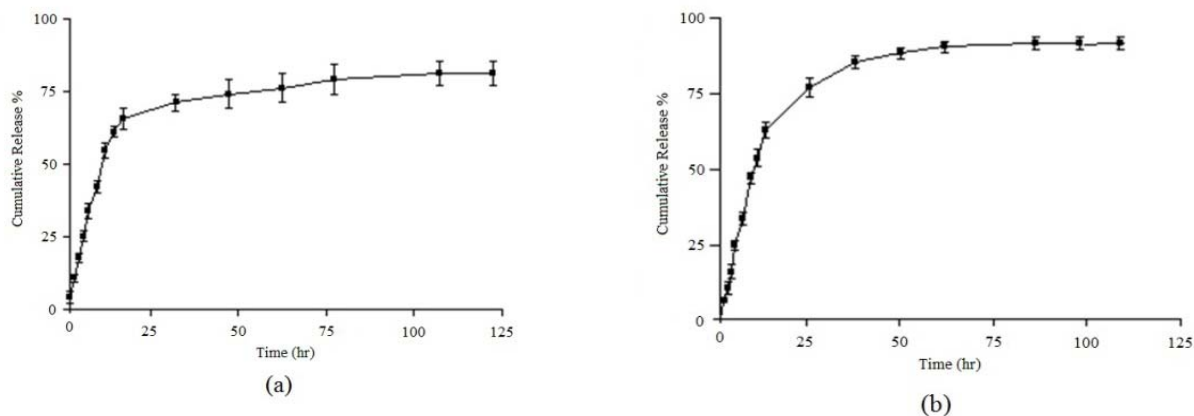

Fig. 7. Cumulative drug released from a; PLGA and b; PLGA-Fol NPs, each value represents the mean of three experiments ± standard deviation.

Table 2. IC$_{50}$ of Free drug, PLGA NP, and PLGA-FOL NPs on cell lines determined by MTT assay.

Formulations	Cell Line				
	MCF-7	HT29	PC3	H9C2	HUVEC
Free Drug	4.7	3.7	4.15	>5	>5
PLGA NP	4.5	3.4	4	>5	4.8
PLGA-FOL NP	1.25	2.84	2.9	>5	4.2

The PLGA thermograms displayed an endothermic peak at 40 ºC which correspons to the polymer transition temperature. The endometric peak appeared at 230 ºC was due to the melting point of 9-NC (16). However, for the 9-NC loaded NPs no melting peak was detected for the drug (22). This suggested that there was no crystalline 9-NC in the NPs, and the drug might be presented in an amorphous state. Furthermore the endometric peak obtained in 140 ºC; corresponds to the folate that was detected in the physical mixture and PLGA-FoA NPs.Using a membrane dialysis method, both PLGA and PLGA-Fol NPs were found to exhibit sustained drug release into PBS medium with a primary slow release of the drug (60% of drug within 10 h) followed by a sustained release of 9-NC .The initial release of the drug could be due to the release of the drug from the PLGA-Fol NPs by a

diffusion mechanism. The initial release was later followed by a more controlled release during 100 h (Fig. 7), which was the result of the drug diffusion and perhaps polymer degradation. Fitting of release data to different kinetic models showed that release exponent (n) derived from Korsmeyer-Peppas equation for the studied formulations implied that this valueranged from 0.46-0.59, indicating that the drug release was mainly governed by diffusion.

In vitro cytotoxic activity

The cell cytotoxicity of 9-NC, PLGA NPs and PLGA-Fol NPs were investigated as shown in Fig. 8. For MCF-7 cells, PLGA-Fol NPs with an IC_{50} (half maximal inhibitory concentration) of 1.25 µg/ml exhibited superior cytotoxic activities than PLGA NPs (IC_{50}=4.5 µg/ml). The folate decorated PLGA NPs significantly decreased the IC_{50} values compared to the free drug on PC3 cell line after incubation for 24 h (2.9 vs 4.15 µg/ml) (Table 2).

On the other hand, for the HUVEC cells, IC_{50} value of PLGA-Fol NPs (4.2 µg/ml) and that of PLGA (4.8 µg/ml) were approximately equal.

This reveals that the folate moieties in PLGA-Fol NPs played an important role in enhancing cytotoxic effect and it also appeared that there was cooperative binding between multiple folic acid molecules on the surface of the polymer and multiple folate receptors on the membranes of tumor cells leading to the higher interactions.
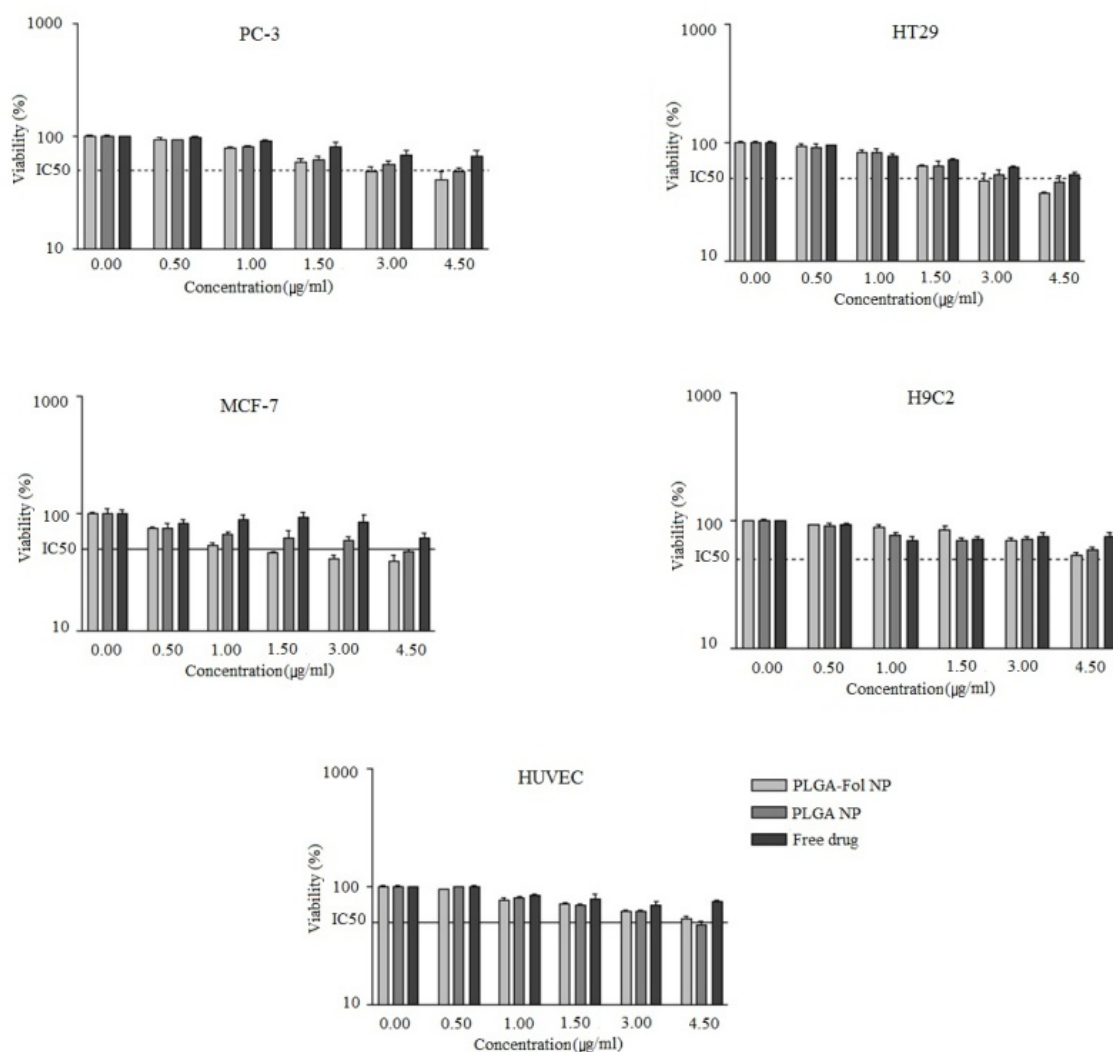

Fig. 8. Cytotoxicity of 9-NC loaded nanoparticles and free drug on different cell lines, each value represents the mean of three experiments ± standard deviation.

DISCUSSION

Active targeting of NPs to specific cells has been proposed through the use of different ligands such as, transferrin receptors, epidermal growth factor receptors (EGFR), folate receptors, human EGFR) 2, integrins, somatostatin/growth hormone receptor and the glucose transporter (7,23). Of the candidates listed, the folate receptor has been extensively explored as a target for cancer treatments.

The following technologies highlight successful and recent folic acid mediated means of nanoparticle uptake for cancer treatment. Folate receptors are highly overexpressed on the surface of many tumor types. This expression can be exploited to target therapeutic compounds directly to cancerous tissues using many avenues.

In the current study we aimed to use folic acid as the targeting agent attached to PLGA for targeting folate receptor binding sites on the surface of cancer cells. Our results confirmed that the folate decorated PLGA NPs exhibited more cytotoxic effect compared to non-targeting NPs. Because it has been reported that many solid tumors, such as ovarian and breast cancers, overexpress the specific receptor for this vitamin, several research groups have developed folate conjugated NPs for targeted delivery of specific agents (24-26).

In a study performed at the Korean Advanced Institute of Science and Technology, the efficacy of nanoscale sized folate receptor-targeted doxorubicin (DOX) aggregates were tested for the treatment of cancer. Their results showed that DOX/Fol nanoaggregates enhanced cellular uptake, increased targeting capacity and also increased cytotoxicity against KB cells over expressing the folate receptors.

In vivo experiment employing human tumor xenograft transplantation in animals also confirmed a superior anti-tumor effect of the folate targeted DOX nano-aggregates (19). In addition, it has been demonstrated that folate targeted solid lipid NPs could significantly enhance the cytotoxic effect of simvastatin on

K562 cell line and also showed synergistic effect with DOX in reducing its dose (27). Moreover, a recent study showed that in a human tumor xenograft nude mouse model, heparin–folic acid–retinoic acid NPs reduced the tumor volume without any signs of toxicity compared to heparin–retinoic acid nanoparticles or free drug (28).

Pan and coworkers developed a new strategy to prepare the folate-decorated NPs of biodegradable polymer for Quantum dots (QDs) formulation in the targeted and sustained imaging for cancer diagnosis at its early stage. The targeted imaging by QDs formulated in folate decorated NPs with better effects and less side effects was obtained (29).

Mansoori and colleagues have reported a cooperative study of two folate conjugated gold NPs using a variety of linkers. This study provides an interesting analysis of the folate receptor tissue distribution and particle endocytosis in the cells with both and low folate receptor expression in cells (Hela and MCF-7, respectively) (30).

As observed in this study, the folate decorated on the surface of PLGA polymer was prepared successfully, and also using nanoprecipitation method, drug was efficiently loaded in the particles.

Free loaded drug showed less cytotoxicity against cell lines compared to PLGA-Fol and PLGA NPs. It could be suggested that the folate receptor-mediated intracellular delivery of 9-NC using folate decorated NPs is an attractive way of circumventing the multidrug resistance and the action of P-glycoprotein efflux pumps.

It should be noted that a relatively short incubation period used in the MTT based cytotoxicity assay (24 h) was not enough to determine a long term cytotoxicity of PLGA-Fol NPs, and a more prolonged incubation time would be required to fully exert the cytotoxicity effect of 9-NC (31,32).

In comparison with other works on this drug, it is suggested that, the drug loaded folate decorated NPs effectively decreased the *in vitro* cancerous cell viability, which could refer to the *in vivo* targeting effects of the NP formulation.

CONCLUSION

In this study, we prepared PLGA-Fol NPs and confirmed their chemical structure by FTIR, ^{1}HNMR spectroscopy, and DSC. PLGA-Fol NPs was used for *in vitro* targeting delivery of 9-NC to the cancer cell lines (HT29, MCF-7, PC3). We found that the PLGA-Fol NPs greatly increased the tumor targeting efficiency and exhibited greater cytotoxic effect compared to the free drug. This study reports a novel technique for the preparation of PLGA-Fol NPs, and also their application in the selective delivery of anticancer drug to the folate receptor-overexpressed cancer cells, which opens a new vista for the site-specific targeting of the anticancer therapy.

ACKNOWLEDGMENTS

REFERENCES

1. Damell JE. Molecular Cell Biology. San Francisco: WH Freeman; 1990. p. 362-333.
2. Cho K, Wang X, Nie S, Chen Z, Shin DM. Therapeutic nanoparticles for drug delivery in cancer. Clin Cancer Res. 2008;14:1310-1316.
3. Crider KS, Yang TP, Berry RJ, Bailey LB. Folate and DNA methylation: a review of molecular mechanisms and the evidence for folate's role. Adv Nutr. 2012;3:21–38.
4. Sudimack J, Lee RJ. Targeted drug delivery via the folate receptor. Adv Drug Delivery Rev. 2000;41:147–162.
5. Thomas TP, Goonewardena SN, Majoros IJ, Kotlyar A, Cao Z, Leroueil PR, *et al.* Folate-targeted nanoparticles show efficacy in the treatment of inflammatory arthritis. Arthritis Rheum. 2011;63:2671–2680.
6. Armstrong DK, White AJ, Weil SC, Phillips M, Coleman RL. Farletuzumab (a monoclonal antibody against folate receptor alpha) in relapsed platinum-sensitive ovarian cancer. Gynecol Oncol. 2013;129:452–458.
7. Garcia-Bennett A, Nees M, Fadeel B. In search of the Holy Grail: folate-targeted nanoparticles for cancer therapy. Biochem Pharmacol. 2011; 81:976-984.
8. Leamon CP, Reddy JA. Folate- targeted chemotherapy. Adv Drug Deliv Rev. 2004;56: 1127–1141.
9. Antony AC. The biological chemistry of folate receptors. Blood.1992;79:2807-2820.
10. Jansen G. Receptor and carrier-mediated transport systems for folates, and antifolates. In: Jackman AL, editor. Antifolate drug in cancer therapy. Totowa NJ: Humana Press; 1999. p. 293-321.
11. Gruner BA, Weitman SD. The folate receptor as a potential therapeutic anticancer target. Invest New Drugs. 1998;16:205–219.
12. Reddy A, Low PS. Folate-mediated targeting of therapeutic and imaging agents to cancers. Crit Rev Ther Drug Carrier Syst. 1998;15:587–627.
13. Lu Y, Low PS. Folate-mediated delivery of macromolecular anticancer therapeutic agents. Adv Drug Deliv Rev. 2002;54:675–693.
14. Chugh R, Dunn R, Zalupski MM, Biermann JS, Sondak VK, Mace JR, *et al.* Phase II study of 9-nitro-camptothecin in patients with advanced chordoma or soft tissue sarcoma. J Clin Oncol. 2005;23:3597-3604.
15. Giovanella BC, Stehlin JS, Hinz HR, Kozielski AJ, Harris NJ, Vardeman DM. Preclinical evaluation of the anticancer activity and toxicity of 9-nitro-20(*S*)-camptothecin (Rubitecan). Int J Oncol. 2002; 20:81–88.
16. Derakhashandeh K, Haghkhah M, Amiri M. Study of the copolymer structure effect on physicochemical characteristics and *in vitro* stability of PLGA–PEG nanoparticles loaded 9-nitrocamptothecin. J Rep Pharm Sci. 2012;1:107-117.
17. Derakhshandeh K, Erfan M, Dadashzadeh S. Encapsulation of 9-nitrocamptothecin, a novel anticancer drug, in biodegradable nanoparticles: Factorial design, characterization and release kinetics. Eur J Pharm Biopharm. 2007;66:34-41.
18. Dadashzadeh S, Derakhshandeh K, Shirazi FH. 9-nitrocamptothecin polymeric nanoparticles: cytotoxicity and pharmacokinetic studies of lactone and total forms of drug in rats. Anticancer Drugs. 2008;19:805-811.
19. Yoo HS, Park GT, Folate-receptor-targeted delivery of doxorubicin nano-aggregates stabilized by doxorubicin–PEG–folate conjugate. J control release. 2004;100:247-256.
20. Shoaib MH, Tazeen J, Merchant HA, Yousuf RI. Evaluation of drug release kinetics from ibuprofen matrix tablets using HPMC. Pak J Pharm Sci. 2006;19:119–124.
21. Park J, Fong PM, Jing L, Russel KS, Booth CJ, Mark Saltzman W, *et al.* PEGylated PLGA nanoparticles for the improved delivery of doxorubicin. Nanomedicine. 2009;5:410-418.
22. Kashanian S, Hemati Azandaryani A, Derakhshandeh K. New surface modified solid lipid nanoparticles using N-glutarylphosphatidyl ethanolamine as the outer shell. Int J Nanomedicine. 2011;6:2393–2401.

23. Sinha R, Kim G, Nie S, Shin D. Nanotechnology in cancer therapeutics: bioconjugated nanoparticles for drug delivery. Mol Cancer Ther. 2006;5: 1909-1917.

24. Ohe Y, Niho S, Kakinuma R, Kubota K, Matsumoto T, Ohmatsu H, *et al*. Phase I studies of cisplatin and docetaxel administered by three consecutive weekly infusions for advanced non-small cell lung cancer in elderly and non-elderly patients. Jpn J Clin Oncol. 2001;31:100-106.

25. Avgoustakis K, Beletsi A, Panagi Z, Klepetsanis P, Livanious E, Evangelatos G, *et al*. Effect of copolymer composition on the physicochemical characteristics, *in vitro* stability, and biodistribution of PLGA–mPEG nanoparticles. Int J Pharm. 2003;259:115-127.

26. Tebarzad M, Rouhani H, Amini M, Dinarvand R. Synthesis of PEGylated zinc protoporphyrin conjugated with folate: For targeted cancer therapy. Res Pharm Sci. 2012;7:S273.

27. Varshosaz J, Hassanzadeh F, Sadeghi H, Shakery M. Folate targeted solid lipid nanoparticles of simvastatin for enhanced cytotoxic effects of doxorubicin in chronic myeloid leukemia. Curr Nanosci. 2014;8:249-258.

28. Oh I, Cho KJ, Tran TH, Huh KM, Lee Y. Biofunctional nanoparticle formation and folate-targeted antitumor effect of heparin-retinoic acid conjugates. Macromol Res. 2012;20:520-527.

29. Pan J, Feng SS. Targeting and imaging cancer cells by folate-decorated, quantum dots (QDs)-loaded nanoparticles of biodegradable polymers. Biomaterial. 2009;30:1176–1183.

30. Mansoori GA, Brandenburg KS, Shakerizadeh A. Comparative study of tow folate-conjugated gold nanoparticles for cancer nanoparticles for cancer nanotechnology applications. Cancer. 2010;2:1911-1928.

31. Sha X, Fang X, Wu Y. The *in vitro* kinetics of uptake, transport and efflux of 9-nitrocamptothecin in Caco-2 cell model. Yao Xue Xue Bao. 2004;39:839-843.

32. Sha X, Fang X. Transport characteristics of 9-nitrocamptothecin in the human intestinal cell line Caco-2 and everted gut sacs. Int J Pharm. 2004;272:161-171.